

An Optimization Framework for Monitor Placement in Quantum Network Tomography

Athira Kalavampara Raghunadhan^{1*}†,
Matheus Guedes De Andrade^{2†}, Don Towsley², Indrakshi Dey³,
Daniel Kilper¹, Nicola Marchetti¹

¹*CONNECT Research Centre, School of Engineering, Trinity College
Dublin, Ireland.

²Manning College of Information and Computer Science, University of
Massachusetts, Amherst, USA.

³Walton Institute, South East Technological University, Waterford,
Ireland.

*Corresponding author(s). E-mail(s): kalavama@tcd.ie;

Contributing authors: mguesdesdeand@umass.edu;
towsley@cs.umass.edu; Indrakshi.Dey@waltoninstitute.ie;
dan.kilper@tcd.ie; nicola.marchetti@tcd.ie;

†These authors contributed equally to this work.

Abstract

Quantum Network Tomography (QNT) offers a framework for end-to-end quantum channel characterization by strategically placing monitor nodes within the network. Building upon prior work on single-monitor placement, we study optimal monitor placement and measurement assignments for channel parameter estimation in arbitrary quantum networks. Using an n -node star network as a baseline, we analyze multi-monitor configurations and show that distributing monitors across end nodes can achieve estimation performance comparable to a monitor placed at the hub. Estimation precision is quantified using the Quantum Fisher Information Matrix (QFIM), with channel parameters inferred via Maximum Likelihood Estimation (MLE) and benchmarked against the Quantum Cramér–Rao Bound (QCRB). To generalize, we develop two Integer Linear Program (ILP) formulations: one maximizing estimation accuracy (QF), and another jointly optimizing accuracy and monitoring overhead (QMF). Unlike QF, QMF prevents monitor overloading, enabling scalability and parallelism. We

prove optimality for star and analyze applicability to tree-structured quantum networks.

Keywords: Quantum Network Tomography, Monitor Placement, Quantum Fisher Information Matrix, Quantum Cramér–Rao Bound, Maximum Likelihood Estimator, Integer Linear Program, Monitoring-overhead.

Introduction

Accurate estimation of quantum channel parameters [1] is essential for reliable quantum communication, particularly in the presence of noise that degrades entangled states during transmission [2]. Quantum Network Tomography (QNT) integrates principles from classical network tomography [3, 4] and quantum tomography to facilitate end-to-end estimation [5, 6] of quantum channels through quantum measurements performed at monitor nodes [7, 8]. In realizable quantum networks where direct access to internal links is often impractical, QNT employs path-based estimation, distributing entangled states across multiple connected links and using entanglement swapping at intermediate nodes to establish end-to-end entanglement between monitor nodes. This enables inference of individual link parameters from end to end measurements, contributing to the development of noise-aware error-correction protocols for reliable quantum communication networks [9, 10].

Earlier studies in QNT [11–14] introduced end-to-end estimation methods for network links, highlighting the importance of optimal monitor placement. Prior work [15] investigated the monitor placement problem in a four-node quantum star network, demonstrating that all network links can be characterized using a single monitor through the proposed probe state distribution and measurement approach under the assumption that communication through network links is affected by depolarizing noise. The findings indicate that the monitors placed at the nodes connected through the least noisy links provide superior estimation performance.

With this foundation in place, this work generalizes the framework in which monitors are not limited to end nodes but may be placed anywhere in the network, with measurement ability independent of their position in the network to handle more intricate configurations and makes the following key contributions.

- We investigate scenarios involving multiple monitors placed at the end nodes of an n -node star network. Theoretical analysis using the Quantum Fisher Information Matrix (QFIM) [16, 17] and the Quantum Cramér–Rao Bound (QCRB) [18] reveals that optimal performance is achieved when monitors are placed at all end nodes, resulting in accuracy comparable to that of a single monitor positioned at the hub [15]. This reaffirms that higher estimation accuracy is obtained for parameters associated with the least noisy links directly connected to nodes with monitors.
- We derive closed-form expressions for the Maximum Likelihood Estimators (MLEs) [19] of the Werner parameters characterizing links in an n -node star network and evaluate their performance against the theoretical lower bound set by the QCRB, observing that the MLE achieves this bound.

- We address the problem of optimal monitor placement in general quantum network topologies by formulating it as an Integer Linear Program (ILP). Our analysis examines two distinct formulations: (i) monitoring-overhead constrained QFIM formulation (QMF), that balances estimation accuracy with monitoring-overhead, and (ii) unconstrained QFIM based formulation (QF) that focuses solely on maximizing estimation accuracy.
- We compare both optimization formulations and observe that the QF approach prioritizes monitor placement on the node incident to highest-quality links, assigning all other links to the monitor deployed on the node associated with top-performing link. This allocation strategy creates a centralized monitoring load, which in turn limits scalability and parallelism. In contrast, the formulation that accounts for both monitoring-overhead and estimation accuracy (QMF) achieves a more balanced distribution of monitoring tasks, thus avoiding excessive overhead associated with a single monitor.
- We provide formal proofs validating the optimal monitoring strategies in star networks for both optimization formulations.
- Finally, the framework is extended and evaluated in tree topologies, where monitoring involves paths that traverse more than two links. The results show that, beyond placing monitors on nodes connected to high-quality links, measurement assignments also prioritize shorter and least noisy paths, providing an additional layer of reliability in estimation.

Results

Probe State Distribution and Measurement

Following our previously established framework [15], we model the network as a graph $G = (V, E)$ where nodes $V = \{v_0, v_1, \dots, v_{n-1}\}$ represent a set of quantum processors and edges $E = \{e_0, e_1, \dots, e_{m-1}\}$ denote the set of quantum channels that interconnect the processors in V . The model assumes that noise is present only during quantum state transmission [20, 21], with each link e_i representing a depolarizing channel [22]. The Werner state $\rho(w_i) = w_i |\Phi^+\rangle\langle\Phi^+| + (1 - w_i) \frac{\mathbb{I}_4}{4}$ [23–25] is used to model entangled states generated through noisy links [26, 27] where $|\Phi^+\rangle = (|00\rangle + |11\rangle)/\sqrt{2}$ and \mathbb{I}_4 is the 4×4 identity matrix. For $w_i = 1$, $\rho(w_i)$ reduces to a pure Bell state, whereas $w_i = 0$ corresponds to the maximally mixed state. Nodes in V are divided into *intermediate* and *monitor* nodes. Intermediate nodes can generate bipartite entanglement with their neighbors and perform entanglement swapping operations to generate end-to-end entanglement. Monitor nodes denoted by $M \subseteq V$ have the same capabilities of intermediate nodes with the additional capability of performing quantum measurements to estimate Werner parameters. The probe state generation process has the objective of generating Werner states at monitor nodes for estimation.

Let $P = \{v_i\}_{i=0}^{q-1}$ be a path connecting the nodes v_0 and v_{q-1} . Each edge $e_i = (v_i, v_{i+1})$ is parameterized by w_i , representing the quality of the link through its connection with entanglement fidelity, $f_\Phi(w_i) = \frac{1+3w_i}{4}$ [14]. To probe the network, we define a probe state as an entangled quantum state generated between two end nodes $v_a, v_b \in V$ by distributing entanglement along a simple path $P_{ab} \subseteq P$ connecting v_a

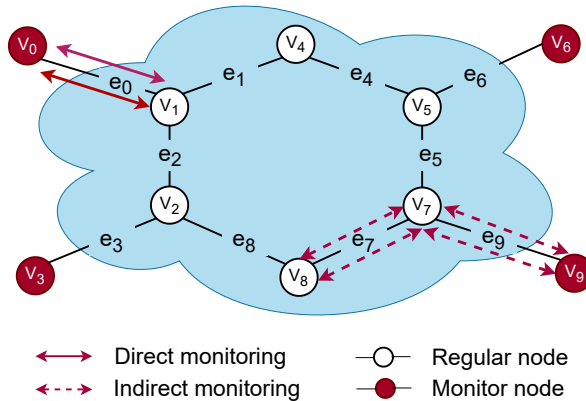


Fig. 1 Probe-state distribution and measurements: Link e_0 is directly monitored by monitor node v_0 , which is an endpoint of the link. Two entangled states are distributed between nodes v_0 and v_1 , shown by solid red arrows. In contrast, link e_7 is indirectly monitored via monitor node v_9 , as it is not incident to any monitor node. In this case, two entangled states are distributed between node pairs (v_8, v_7) and (v_7, v_9) , indicated by dashed red arrows.

and v_b . Let P_{ab} consist of l links. Without loss of generality, assume that a monitor is placed at node v_a . Then, the probe state generation proceeds as follows. Two copies of the Werner state $\rho(w_i)$ are generated between nodes v_a and v_b each using Werner states created across each link on the path P_{ab} followed by Bell State Measurements (BSMs) performed at the intermediate nodes. Once the end-to-end pairs are created, a BSM will be performed at v_b . As a result, the Werner state

$$\rho_{ab} = \rho\left(\prod_{i=0}^{l-1} w_i^2\right) \quad (1)$$

is generated at node v_a . A final BSM is then performed locally at the end node equipped with the monitor, i.e., v_a , yielding classical outcomes that are used for parameter estimation. In this framework, each monitor node v_i measures entangled states distributed across one or more network links. A link $e_i = (v_i, v_j)$ is said to be *directly monitored* by the monitor in node v_i if the entangled pair measured for parameter estimation is distributed exclusively over link e_i , with density matrix given by $\rho(w_i^2)$. If the entanglement is distributed through a multi-link path P containing e_i , the link is considered to be *indirectly monitored* by v_i as illustrated in Fig. 1.

We use the QFIM, valid for arbitrary networks [14–16], to evaluate monitor placement strategies based on the proposed probe state distribution and measurement framework, with complete derivations provided in Supplementary Note 1. The QFIM of the Werner state $\rho(w_i)$ quantifies the amount of information the state carries about the parameter w_i . The QFIM is additive with respect to tensor products such that, when multiple quantum states are used for estimation, the QFIM becomes the entry-wise sum of the QFIMs for each individual state. The QFIM determines the QCRB, which is a lower bound on the variance of any unbiased estimator \hat{w}_i of w_i that can

be obtained from measurements of $\rho(w_i)$. Thus, the QCRB establishes the best possible parameter estimation accuracy that can be achieved in QNT. When a link e_i is *directly monitored* by a monitor node, the contribution to the QFIM appear as a diagonal element given by

$$F_i^D = \frac{12w_i^2}{(1 + 3w_i^2)(1 - w_i^2)}. \quad (2)$$

For *indirect monitoring* of a link e_i through a path P , the QFIM is given by

$$F_{ij}^I = \frac{12w_i w_j \left(\prod_{\substack{l \in P \\ l \neq i}} w_l^2 \prod_{\substack{l \in P \\ l \neq j}} w_l^2 \right)}{(1 + 3 \prod_{l \in P} w_l^2)(1 - \prod_{l \in P} w_l^2)}. \quad (3)$$

Following the QFIM formulation, we estimate the Werner parameters $\{w_i\}$ in a n -node star network using the MLE method [28] which is summarized in the Methods section and derived in detail in Supplementary Note 2.

The Optimal Monitor Placement Problem

The optimal monitor placement problem consists of placing monitors in the network nodes and specifying the probes utilized for QNT such that: (i) Werner parameters for all network links can be estimated and (ii) the solution obtained optimizes a desired measure of estimation performance. We now describe an optimization framework for determining optimal monitor placement for QNT, for which we adopt principles of optimal experimental design. Common approaches [29, 30] include minimizing average variance (A-optimality), maximizing determinant (D-optimality), maximizing trace (T-optimality) and maximizing minimum eigenvalue (E-optimality), each emphasizing different aspects of the QFIM and yielding distinct QNT solutions. In addition to experimental design objectives, we study monitor assignments that balance the monitoring load assigned to network monitors, which is of practical interest.

From a statistical standpoint, there are strong reasons to prefer objectives that operate on the inverse or the determinant of the QFIM. In particular, minimizing the trace of the inverse QFIM, $\text{Tr}(F_Q^{-1})$, where F_Q denotes the quantum Fisher information matrix associated with the estimated parameters, directly targets the aggregate estimation error through the QCRB, as it lower bounds the sum of the variances of any locally unbiased estimator. This makes A-optimality the most transparent measure of estimator quality. Likewise, maximizing determinant of QFIM encourages designs that are informative in all parameter directions by penalizing poorly conditioned matrices, which is the central idea behind D-optimality. In both cases, these objectives provide robust, theoretically grounded measures of statistical performance. However, these are difficult to optimize analytically and numerically. Both matrix inversion and determinant computations introduce nonlinear and nonconvex expressions in the decision variables, which makes the resulting problem extremely hard to solve when monitor

placement decisions are binary. Incorporating these operations into an ILP either renders the model intractable or requires relaxations that undermine the exactness of the solution.

In this work, to maintain scalability, we adopt the T-optimal criterion [31], since maximizing the trace of the QFIM maximizes the sum of the QFI for all parameters. The trace grows with the total amount of information contributed by all measurements and, importantly, depends linearly on the variables that encode the monitor placement problem. This allows formulating the monitor placement problem as an ILP since nonlinear constraints are absent. While A-optimality (minimizing $Tr(F_Q^{-1})$) targets aggregate error directly, it is computationally intractable for ILP due to non-linearity and non-convexity. Although T-optimality is a simpler metric than A- or D-optimality, it is widely used as a practical surrogate because it tends to improve estimator precision while keeping the optimization problem manageable [32–34]. However, T-optimality does not directly quantify estimation error. After solving the ILP using this surrogate objective, we evaluate the resulting designs using the inverse trace of the QFIM which lower bounds the total estimation variance via the QCRB and thus provides a more meaningful measure of practical estimation performance.

We propose two ILP formulations for the optimal monitor placement problem: one that maximizes the trace of the QFIM (QF), and another that obtains the maximum achievable QFIM trace under constraints on the number of links monitored by each network monitor (QMF). The first solution prioritizes estimation accuracy, while the second solution balances accuracy with parallel probe generation, i.e., the simultaneous use of multiple probe paths. We now provide a detailed description of the objective terms, the decision variables, and the constraints that define the solution space.

Table 1 List of Variables

Variables	Description
V	Set of network nodes (Vertices)
E	Set of network links (Edges)
M	Set of monitors
F_i^D	Direct QFIM contribution
$F_{i,j}^I$	Indirect QFIM contribution
$x_{i,j}$	Link i is directly measured by monitor j
$p_{i,j}$	Link i is indirectly measured by monitor j
$m_{k,j}$	Monitor j is placed at node k
$y_{i,j}$	Monitor j indirectly monitors i if a learnable path connects i to j
b_i	Link i is learnable by any monitor
l_j	Number of links measured by monitor j
L_j^*	Monitoring capacity of monitor j

QMF and QF ILP Formulation

We now present the ILP formulation for QMF, which solves the monitor placement problem by maximizing the QFIM trace under monitor capacity constraints. The QF ILP formulation is obtained by removing constraints from the formulation presented.

The goal of QMF is to jointly maximize the estimation accuracy of quantum measurements and minimize the measurement overhead on individual monitors. To capture this trade-off, the objective function maximizes the trace of the QFIM, i.e., total QFI contained in probes for both direct and indirect measurements, subject to monitor-specific capacity constraints. The capacity of a monitor corresponds to the maximum number of links the monitor can measure. Direct measurements of a link can only occur when a monitor is located at one end node of that link. Indirect measurements require a closed probe path that starts and ends at a monitor node and traverses the target link. In a star topology, this corresponds to a four-hop cycle through the hub. The decision variable $x_{i,j} \in \{0, 1\}$ denotes whether monitor j directly measures link i , while $p_{i,j} \in \{0, 1\}$ indicates indirect measurement of link i by monitor j . Also, the placement of the monitor j on node k is represented by the decision variable $m_{k,j}$. To compute the trace of the final QFIM, we sum the diagonal elements of the QFIM corresponding to direct monitoring $F_i^{(D)}$, and the QFIM corresponding to indirect monitoring $F_{ij}^{(I)}$, where each term is weighted by the corresponding decision variables to reflect the actual monitor placement and measurements. The measurement overhead of a monitor is the total number of links that are either directly or indirectly measured by the monitor, and the monitoring-overhead is the maximum measurement overhead among all deployed monitors. The optimization formulation is defined as follows,

$$\max_{x_{i,j}, p_{i,j}, m_{k,j}} \sum_{\substack{i \in E \\ j \in M}} (x_{i,j} F_i^{(D)} + p_{i,j} F_{ij}^{(I)}). \quad (4)$$

s.t.

$$\sum_{j \in M} (x_{i,j} + p_{i,j}) = 1, \quad \forall i \in E; \quad (5)$$

$$x_{i,j} \leq m_{k_1(i),j} + m_{k_2(i),j}, \quad \forall k_1, k_2 \in V, i \in E, j \in M; \quad (6)$$

$$\sum_{j \in M} x_{i,j} = \min \left(1, \sum_{j \in M} (m_{k_1(i),j} + m_{k_2(i),j}) \right), \quad \forall k_1, k_2 \in V, i \in E, j \in M; \quad (7)$$

$$b_i \geq \frac{1}{2|M|} \sum_{j \in M} (x_{i,j} + y_{i,j}), \quad \forall i \in E; \quad (8)$$

$$y_{i,j} \leq \frac{1}{|\mathcal{P}_{k,i}|} \left(\sum_{h \in \mathcal{P}_{k,i}} b_h \right) + p_{i,j} + (1 - m_{k,j}), \quad \forall i \in E, \forall j \in M, \forall k \in V; \quad (9)$$

$$\sum_{k \in V} m_{k,j} = 1, \quad \forall j \in M; \quad (10)$$

$$\sum_{j \in M} m_{k,j} \leq 1, \quad \forall k \in V; \quad (11)$$

$$\ell_j = \sum_{i \in E} (x_{i,j} + p_{i,j}) \quad \forall j \in M; \quad (12)$$

$$\ell_j \leq L_j^*, \quad \forall j \in M; \quad (13)$$

$$x_{i,j} \in \{0, 1\}, \quad \forall i \in E, j \in M; \quad (14)$$

$$p_{i,j} \in \{0, 1\}, \quad \forall i \in E, j \in M; \quad (15)$$

$$m_{k,j} \in \{0, 1\}, \quad \forall k \in V, j \in M; \quad (16)$$

$$b_i \in \{0, 1\}, \quad \forall i \in E; \quad (17)$$

$$y_{i,j} \in \{0, 1\}, \quad \forall i \in E, j \in M; \quad (18)$$

$$\ell_j \geq 0. \quad (19)$$

Prior to solving the optimization problem, all feasible monitoring paths are generated in a pre-processing step. Specifically, for the given topology $G = (V, E)$, and for every candidate monitor location $k \in V$ and target link $i = (u, v) \in E$, we compute the unique hop-shortest path from node k to node u and append edge (u, v) to obtain the routing path $\mathcal{P}_{k,i}$.

Constraint (5) ensures that each link is measured exactly once, either directly or indirectly by a monitor. Constraint (6) allows direct measurement of a link if, and only if, a monitor is placed at one of the endpoints of that link and Constraint (7) prevents the over-counting of direct measurements when both nodes at the ends of a link are equipped with monitors. A link is considered learnable if its Werner parameter can be estimated from the probe states used for tomography. Constraint (8) specifies that a link $i \in E$ is learnable if: (i) it is measured directly by any monitor or (ii) there exists a path connecting i to a monitor j such that all links in the path are learnable and j monitors i indirectly. Constraint (9) ensures that Condition (ii) is satisfied. This formulation ensures that link parameters can be estimated for every network link and is applicable to arbitrary network topologies.

Constraints (8) and (9) allow a link $i \in E$ to be indirectly monitored by monitor j even if the links in the path between the node containing j and i are indirectly monitored by monitors different than j . If this behavior is not desired, the constraint

$$p_{i,j} \leq \frac{1}{|\mathcal{P}_{k,i}|} \sum_{h \in \mathcal{P}_{k,i}} (x_{h,j} + p_{h,j}) + (1 - m_{k,j}), \quad \forall i \in E, \forall j \in M, \forall k \in V; \quad (20)$$

replaces Constraints (8) and (9) to ensure that link i can be indirectly monitored by j if, and only if, all links along the path connecting j to i are measured either directly or indirectly by j .

Furthermore, Constraint (10) assigns each monitor to one node, while constraint (11) limits each node to have at most one monitor. Finally, (12) defines the measurement overhead ℓ_j for each monitor j as the total number of links assigned to it for both direct and indirect measurement, and (13) upper-bounds the measurement overhead of monitor j by its monitoring capacity L_j^* . This formulation allows monitors to

have different capacities, which is of practical interest. In the remainder of this work, we assume all monitors have the same capacity, i.e., $L_j^* = L^*$. From the definition of monitoring-overhead, $\lceil (n - m)/m \rceil + 1 \leq L^* \leq n$. This formulation supports parallel probe generation when $L^* < n$ and distributes the measurement overhead across monitors.

The objective of the QF optimization problem is to maximize estimation accuracy and is obtained by omitting constraints (12), (13), and (19) from the QMF formulation. In this case, the optimization problem is focused on the T-optimality criteria from experimental design and often leads to monitor overloading where a single node handles all tasks. This justifies the QMF problem formulation.

Optimality in Star Networks

The ILP formulation presented previously is applicable to arbitrary networks. Solving the ILP can be impractical, depending on the number of nodes and edges in a network. We now present an algorithm for star networks that computes the monitoring strategy significantly faster than solving the ILP.

Let G be a star network with n links, each associated with a Werner parameter $w_i \in [0, 1]$, for $i = 1, 2, \dots, n$. Assume, without loss of generality, that the Werner parameters are ordered such that $w_i \geq w_{i+1}$, for $i = 1, \dots, n - 1$. Let $m \leq n$ denote the number of monitors deployed in the network. We place monitors at the m nodes incident to the links with the m largest Werner parameters. Every link is either *directly monitored* or *indirectly monitored*. Let $L^* \in \mathbb{N}$ denote the monitoring-overhead constraint for a monitor placement in G , such that $\lceil (n - m)/m \rceil < L^* \leq n$. The number of monitors that must perform indirect monitoring to satisfy this constraint L^* is $M^* = \lceil n/L^* \rceil$, which can be smaller than m . Let C^* denote the number of links that must be indirectly monitored to satisfy the monitoring-overhead constraint L^* . Let $C_{\text{ind}} := (L^* - 1)$ denote the indirect-link assignment capacity. Let L_j denote the set of links that are indirectly monitored by monitor j . Let $P_{m, L^*}^n = \{L_1, \dots, L_{M^*}\}$ denote a partition of the links $\in C^*$, such that:

1. if $e_1 \in L_i$ and $e_2 \in L_j$, $1 \leq i < j < M^*$, then $w_{e_1} \geq w_{e_2}$
2. the number of links in L_i is $|L_i| = C_{\text{ind}}$, for $i = 1, \dots, (M^* - 1)$;
3. the number of links in L_{M^*} is $|L_{M^*}| = C^* - C_{\text{ind}}(M^* - 1)$.

The partition P_{m, L^*}^n directly specifies a monitoring strategy for all links in the star network with monitoring-overhead L^* , which is given by Algorithm 1. The set L_j contains the links that are indirectly monitored by monitor j , and the link with Werner parameter w_j is directly monitored by monitor j , for $j = 1, \dots, M^*$.

The runtime of Algorithm 1 is $O(n \log n)$, which is dominated by sorting links based on their Werner parameters. We now establish the optimality of Algorithm 1 through a series of lemmas that culminate in Theorem 1. Note that the ordering imposed by condition 1 in the definition of P_{m, L^*}^n is key to its optimality. From Eq. (2), the Quantum Fisher information (QFI) F_i^D corresponding to the direct monitoring of link i is

$$F_i^D = \frac{12w_i^2}{(1 + 3w_i^2)(1 - w_i^2)}. \quad (21)$$

Algorithm 1 Optimal monitoring strategy for star networks

Require: $G = (V, E)$; m ; $\{w_i\}$; L^* .

Ensure: Optimal monitoring strategy.

- 1: Sort links by decreasing order of Werner parameters.
 - 2: Construct partition $P_{m, L^*}^n = \{L_1, \dots, L_{M^*}\}$.
 - 3: **for** $i = 1, \dots, m$ **do**
 - 4: Place monitor i in node incident to link e_i .
 - 5: Monitor link e_i directly with monitor i .
 - 6: **if** $|L_i| \geq 0$ **then**
 - 7: Monitor links in L_i indirectly through monitor i .
 - 8: **end if**
 - 9: **end for**
-

From Eq. (3), the QFI corresponding to the indirect monitoring of link j through link i is

$$F_{ij}^I = \frac{12w_i^2w_j^4}{(1 + 3w_i^2w_j^2)(1 - w_i^2w_j^2)}. \quad (22)$$

Lemma 1 *If $w_i \geq w_j$, then directly monitoring link i yields at least as much QFI as directly monitoring link j , i.e.,*

$$F_i^D \geq F_j^D. \quad (23)$$

Proof The lemma is proved by showing that $\Delta_F^{ij} = F_i^D - F_j^D \geq 0$ when $w_i \geq w_j$. See supplementary note 3 for the complete algebraic derivation. \square

Lemma 2 *For any link i , direct monitoring yields greater QFI than indirect monitoring, i.e.,*

$$F_i^D \geq F_{ik}^I, \quad (24)$$

for any $k \neq i$.

Proof Similar to the proof for Lemma 1, this Lemma is proved by showing that $\Delta_F^{ik} = F_i^D - F_{ik}^I \geq 0$ for all k . Algebraic manipulations on (21) and (22) allows showing that the denominator of Δ_F^{ik} is

$$12w_i^2(1 - w_k^4) + 24w_i^4w_k^2(1 - w_k^2) \geq 0. \quad (25)$$

The proof shows that the difference Δ_F^{ik} is non-negative because $12w_i^2(1 - w_k^4) + 24w_i^4w_k^2(1 - w_k^2) \geq 0$. This reinforces why the QF (unconstrained) will always prefer direct monitoring when possible. See supplementary note 3 for the complete algebraic derivation of (25). \square

Lemma 3 *If $w_i \geq w_j$, then indirect monitoring of link k through a monitor incident to link i produces at least as much QFI as indirect monitoring through a monitor incident to link j , i.e.,*

$$F_{ik}^I \geq F_{jk}^I. \quad (26)$$

Proof When $w_i \geq w_j$ and $w_i, w_j, w_k \in [0, 1]$, algebraic manipulations allow us to show that the numerator of $\Delta_F^{ijk} = F_I^{ik} - F_I^{jk}$ is

$$(w_i^2 - w_j^2)[12w_k^4 + 36w_i^2w_j^2w_k^8] \geq 0, \quad (27)$$

and that its denominator is also non-negative. See supplementary note 3 for the complete algebraic derivation of (27) \square

Lemma 4 *If $w_i \geq w_j$, then direct monitoring of link i and indirect monitoring of link j through a monitor incident to link i yields at least as much QFI as direct monitoring of link j and indirect monitoring of link i through a monitor incident to link j , i.e.,*

$$F_i^D + F_{ij}^I \geq F_j^D + F_{ji}^I \quad (28)$$

Proof This Lemma is proved by showing that

$$(F_i^D - F_j^D) + (F_{ij}^I - F_{ji}^I) \geq 0, \quad (29)$$

For $0 \leq w_i, w_j < 1$, both the numerator and denominator of the above expression remain non-negative, ensuring that the inequality holds. This lemma provides a mathematical justification for placing monitors at nodes incident to the highest-quality links and bridges the gap between individual link estimation and network-wide trace maximization. The complete algebraic derivation of (29) is provided in supplementary note 3. \square

Lemma 5 *Let links i, j, a, b satisfy $w_i \geq w_j \geq w_a \geq w_b$. Then the total QFI of the sorted indirect assignments dominates that of the crossed assignments:*

$$F_{ia}^I + F_{jb}^I \geq F_{ib}^I + F_{ja}^I. \quad (30)$$

Proof We prove this lemma by demonstrating that

$$(F_{ia}^I + F_{jb}^I) - (F_{ib}^I + F_{ja}^I) \geq 0, \quad (31)$$

Under conditions $0 \leq w_i, w_j, w_a, w_b < 1$, both the numerator and denominator remain non-negative, thereby ensuring the validity of the inequality. This lemma justifies the ‘‘sorted’’ assignment strategy. It proves that pairing better monitors with better indirect links yields a higher total QFI than ‘‘crossing’’ them. The full derivation of (31) is presented in supplementary note 3. \square

Theorem 1 (L^* -constrained QFIM-based Optimality in Star Networks) *The monitor placement that maximizes the trace of the QFIM of the Werner parameters in G with a monitoring-overhead of L^* is to place monitors on the m nodes incident to the links with the m largest Werner parameters $w_1 \geq \dots \geq w_m$. The optimal monitoring strategy follows the partition P_{m, L^*}^n such that:*

1. the link with parameter w_j is directly monitored by monitor j , for $j = 1, \dots, m$;
2. links in L_j are indirectly monitored by monitor j through the link with parameter w_j , for $j = 1, \dots, M^*$.

Proof We prove Theorem 1 via three exchange arguments: one related to the placement of the m monitors in the nodes incident to the links with the m highest Werner parameters; one related to Condition 1 in the definition of the partition P_{m,L^*}^n ; and one related to Conditions 2 and 3 in the definition of the partition P_{m,L^*}^n .

Monitor placement. Assume that a monitor is placed on node v_j , with $j > m$. Since there are m monitors, there exists a node $v_i < v_j$ with $i < j$ and no monitor, although $w_i \geq w_j$. Since no monitor resides in v_i , link e_i is monitored indirectly. Without loss of generality, let this monitor be the one placed in node v_k . Let $P' = \{L'_1, \dots, L'_{i-1}, L'_j, L'_{i+1}, \dots, L'_{M^*}\}$ denote the partition of indirectly monitored links related to this placement strategy, where L'_l is the set of links indirectly monitored by the monitor in node v_l , with $l = 1, \dots, i-1, j, i+1, \dots, M^*$. The only requirement on the partition P' is that $|L'_l| \leq C_{ind}$ for every l , what enforces that the overhead of the corresponding monitoring strategy is $L^* = C_{ind} + 1$.

We now present an exchange operation that generates a new partition P'' from P' with strictly higher QFIM's trace. Let $P'' = \{L''_1, \dots, L''_{M^*}\}$ be the partition obtained by changing the monitor from v_j to v_i such that:

1. $L''_i = L'_j$,
2. $L''_k = (L'_k \setminus \{e_i\}) \cup \{e_j\}$, and
3. $L''_l = L'_l$ for $l \notin \{i, j, k\}$.

It follows from Lemmas 1 through 4 that $\text{Tr}[F_{P''}] > \text{Tr}[F_{P'}]$. Since $|L''_l| \leq C_{ind}$, the monitoring-overhead of the partition P'' is L^* .

Link ordering. The exchange argument presented for the placing of monitors ensures that the optimal partition has monitors placed on the nodes incident to the links with the m highest Werner parameters. Now we present an exchange argument that ensures that Condition 1 in the definition of P_{m,L^*}^n is optimal. Let $P' = \{L'_1, \dots, L'_{M^*}\}$ denote a partition where monitors are placed in the nodes incident to the links with the m highest Werner parameters, with $|L'_l| \leq C_{ind}$ for all l . Assume that there exists a link $e_a \in L_j$ and $e_b \in L_i$, with $w_i > w_j > w_a > w_b$. Let $P'' = \{L''_1, \dots, L''_{M^*}\}$ denote a partition with

1. $L''_i = (L'_i \setminus \{e_b\}) \cup \{e_a\}$,
2. $L''_j = (L'_j \setminus \{e_a\}) \cup \{e_b\}$, and
3. $L''_l = L'_l$ for $l \notin \{i, j\}$.

From Lemma 5, $\text{Tr}[F_{P''}] > \text{Tr}[F_{P'}]$. Since $|L''_l| \leq C_{ind}$ for all l , the monitoring-overhead of P'' is L^* .

Cardinality of sets of indirectly monitored links. The final piece to complete the proof of Theorem 1 is to show that Conditions 2 and 3 in the definition of the partition L_{m,L^*}^n are optimal. For this, consider a partition $P' = \{L'_1, \dots, L'_{M^*}\}$ for which there exists i and j such that $|L'_i| < |L'_j| \leq C_{ind}$. Consider a new partition $P'' = \{L''_l\}_{l=1}^{M^*}$ with $L''_l = L'_l$ for $l \notin \{i, j\}$, $L''_i = L'_i \cup \{e_a\}$, $L''_j = L'_j \setminus \{e_a\}$, and $e_a \in L'_j$ is any link indirectly monitored by monitor j . From Lemma 3, $\text{Tr}[F_{P''}] > \text{Tr}[F_{P'}]$. By construction, the monitoring-overhead of P'' is not greater than L^* .

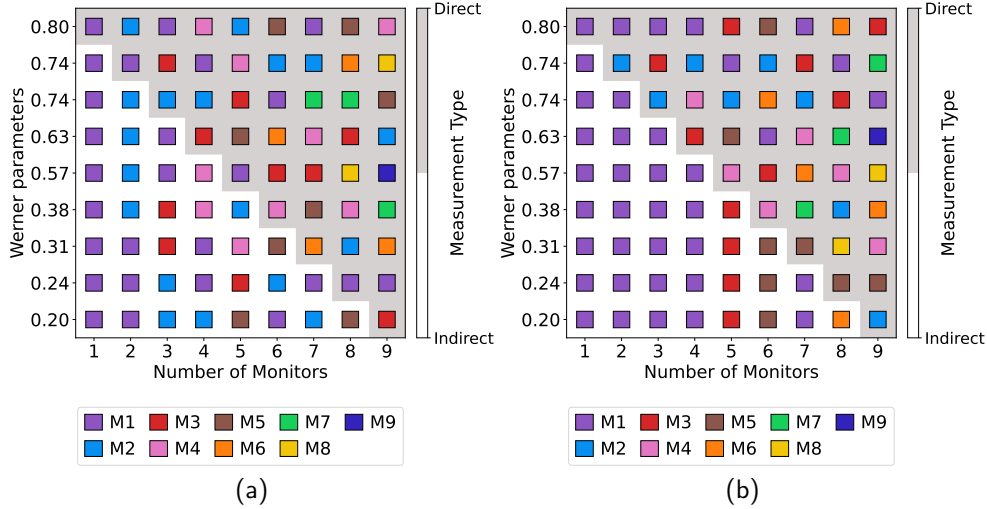


Fig. 2 Monitor placement results for a 10-node star network with nine available monitors. The x-axis indicates the number of deployed monitors from 1 to 9, and the y-axis lists the network links in descending order of their corresponding Werner parameter values. Indirectly measured links are shown in white, while directly measured links are represented in light gray. Distinct colors within each cell represent the specific monitor responsible for the measurement. Subfigures illustrate results from (a) QMF, (b) QF.

The partition P_{m,L^*}^n is invariant with respect to the three exchange arguments provided. Thus, the partition maximizes the trace of the QFIM and is optimal for the monitoring-overhead constraint L^* . \square

Corollary 1 (Unconstrained QFIM based Optimality in Star Networks) *The optimal monitoring strategy that maximizes the trace of the QFIM of the Werner parameters in G without a monitoring-overhead constraint, i.e., monitoring capacity is unbounded for all monitors, on the estimation process is obtained by:*

1. placing the m monitors on the nodes incident to the m links $\{e_1, \dots, e_m\}$ with the largest Werner parameters $w_1 \geq \dots \geq w_m$;
2. directly monitoring each link e_i with the monitor at its incident node, for $i = 1, \dots, m$;
3. indirectly monitoring all remaining links $\{e_{m+1}, \dots, e_n\}$ through the monitor incident to the link with the largest Werner parameter w_1 .

Justification. This result follows directly from Theorem 1 by setting $L^* = n$, for which the monitoring-overhead constraint, (13), becomes trivial and $M^* = 1$.

Evaluation in Star Network

We now evaluate the QMF and QF ILP formulations, i.e., with and without constraints (12), (13), and (19), in a 10-node star network. Fig. 2a presents the monitor placement

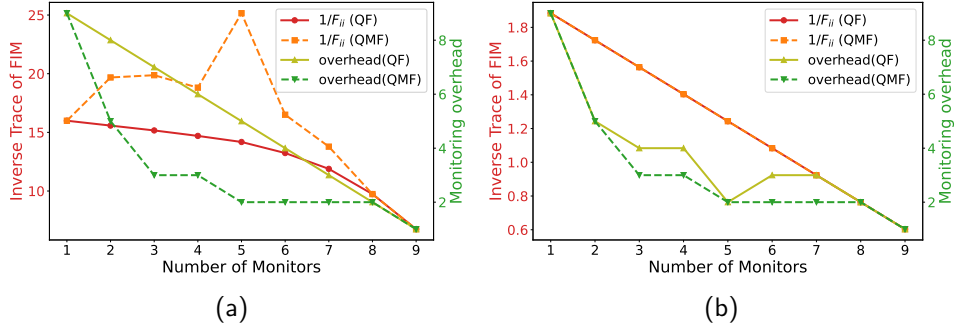


Fig. 3 Comparison of QMF and QF for the Star Network: (a) Both formulations under Heterogeneous noise, (b) Both formulations under uniform noise and estimator value set to 0.9.

in QMF for monitor counts ranging from 1 to 9. With two monitors, the nodes adjacent to the two best links in the network—the two monitors with the highest Werner parameters—are selected for monitor placement. The remaining seven links are then allocated such that four are monitored by M_1 and three by M_2 . With three monitors M_1, M_2 , and M_3 , the six links that are not directly connected to a monitor are evenly distributed, with each monitor assigned two links. This behavior continues to be observed as we increase the number of monitors up to nine, when every network link is directly monitored.

Fig. 2b shows the direct and indirect measurement assignments across network links for the QF approach. When only one monitor is available, the optimal strategy is to place the monitor in the node adjacent to the link with the highest Werner parameter, estimate that link directly, and estimate all other links indirectly through two-hop paths that contain the link with the highest Werner parameter. As additional monitors are deployed, the optimal strategy assigns them by prioritizing links with higher Werner parameters. By the time nine monitors are deployed, full direct coverage is achieved. In the case of indirect measurements, the formulation consolidates all assignments onto the monitor placed at the node incident to the link with the highest Werner parameter, thereby overloading a single monitor.

We evaluate both ILP formulations by comparing their QCRBs, i.e., the trace of the QFIMs inverse, and monitoring-overhead values in both homogeneous and heterogeneous noise settings. Figs. 3a and 3b present the comparison results as the number of deployed monitors increases from 1 to 9.

In the heterogeneous noise scenario, where the underlying Werner parameters vary across links, the QMF approach consistently incurs lower monitor overhead compared to the QF approach by distributing the monitoring load more evenly across the network. However, this improvement in overhead comes at the cost of increased estimation error, as seen from the higher inverse trace of the QFIM. This indicates that forcing a balanced load can actually reduce the total information gathered by the network. This trade-off arises because, in the presence of heterogeneous noise, some links contribute more significantly to the total QFI than others. The QF approach prioritizes assigning monitors to such high-quality links, optimizing precision without regard for load

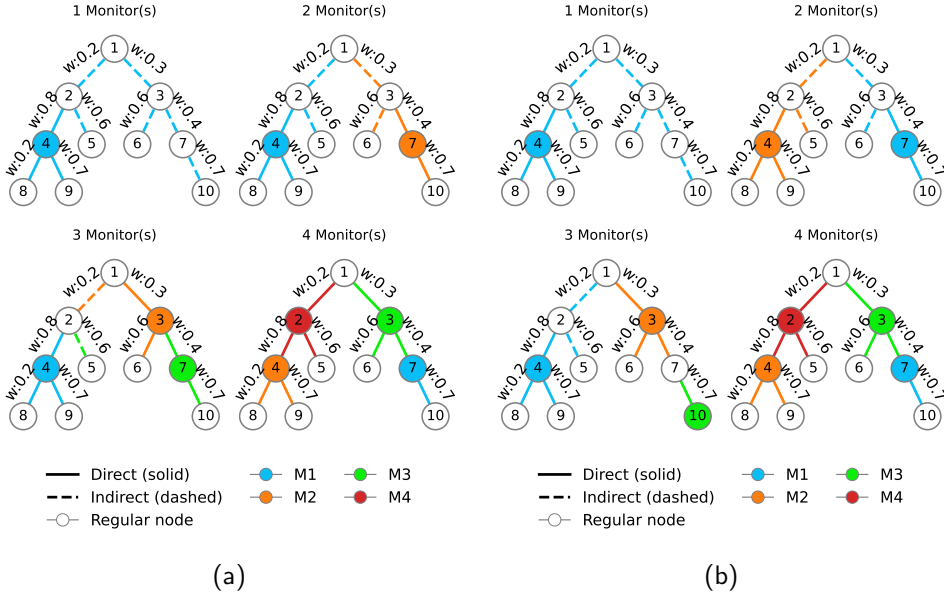


Fig. 4 Monitor placement results for the 10-node tree network with up to four monitors. Node colors indicate monitor placements, and edge colors reflect the monitor performing the measurement. Solid edges denote links that are directly measured, while dashed edges represent indirect measurements. All links in the tree can be directly measured using four monitors, represented by four distinct colors, with each edge color corresponding to the monitor (of the same color) responsible for measuring that link. Subfigures show results from (a) QMF (b) QF.

balance. In contrast, the QMF formulation includes a monitoring-overhead constraint, which discourages monitor overloading. As a result, measurements can be reassigned from high-quality links to lower-quality ones simply to reduce the per-monitor load, leading to suboptimal estimation performance in terms of precision.

In contrast, under homogeneous noise conditions, where all link parameters are identical, both formulations yield identical inverse trace values across all monitor counts. However, QMF consistently provides lower monitor overhead, demonstrating its advantage in reducing resource usage without significantly compromising estimation quality. In this specific case, QMF is strictly superior because it achieves the same precision as QF but with lower resource overhead.

The choice of formulation ultimately depends on the network requirement. The QMF approach is particularly suitable for practical implementations where monitor resources are constrained or load balancing across the network is critical. In contrast, the QF formulation becomes more meaningful when prioritizing estimation accuracy, especially under heterogeneous noise conditions.

Numerical Analysis of Tree Networks

We further showcase the applicability of our optimization formulations by extending our analysis to a 10-node tree topology with inhomogeneous noise, solving both the

QF and QMF formulations when varying the number of monitors from one to four. The variation in monitor ordering is due to symmetry in the model, as all monitors are identical and interchangeable.

Fig. 4a presents the outcomes of the QMF, which distributes the monitoring load more evenly across available monitors while still prioritizing high-quality paths. With three monitors, nodes 4, 3, and 7 are selected, covering the highest Werner parameters regions of the network while ensuring that no single monitor is overloaded. This behavior follows directly from the QMF objective. With four monitors, all links can be directly monitored and the allocation becomes nearly uniform, confirming that the formulation balances estimation accuracy with measurement overhead in hierarchical structures.

Fig. 4b reports the results for the QF approach on the same topology used to analyze the QMF. In this formulation, monitor placement is dominated by path quality, as the objective maximizes the total QFIM trace without accounting for monitor load. As a result, monitors are placed at the nodes connected to the links with the highest Werner parameters, where additional path assignments consistently improve the objective value. Although this strategy achieves high estimation precision, it leads to pronounced load concentration, with many remaining links being assigned indirectly through the same monitor connected to the best-quality link, thereby limiting scalability. For example, placing three monitors at nodes 4, 3, and 10 yields the maximum QFIM trace but assigns five links to monitor $M1$, compared to only three links assigned to $M1$ under the QMF for the same configuration.

The results for the tree network reveal a key distinction between the two formulations. Under the QF approach, the optimization prioritizes monitor placement that minimizes path length and noise, which in some cases (e.g., two monitors) leads to an approximately balanced distribution. In such cases, the balance arises as a byproduct of the network topology rather than an explicit objective. In contrast, the QMF explicitly encourages a more uniform distribution of monitoring tasks across the network. For further comparison, the results for the tree topology obtained by replacing Constraints (8) and (9) with the Constraint (20) are reported in Supplementary Note 4.

Methods

Werner Parameter Estimation

The maximum likelihood estimator \hat{w}_i represents the estimated value of the link parameter w_i that maximizes the likelihood of the observed measurement outcomes. Due to its asymptotic efficiency, MLE ensures that as the number of measurements increases, the variance of the estimator \hat{w}_i approaches the QCRB limit, thus achieving optimal precision in the large-sample regime.

The MLE, \hat{w}_i derived for the *direct monitoring* of the link e_i in a star network of arbitrary size is represented in the following Eq. (32).

$$\hat{w}_i = \sqrt{\frac{4N_{00_i} - N_i}{3N_i}} \quad (32)$$

where N_{00_i} denotes the number of measurement outcomes of state ϕ_{00} corresponding to link e_i and N_i represents the total number of measurements performed on e_i .

In the *indirect monitoring* scheme, two distinct estimators are used. Estimator \hat{w}_i corresponds to link e_i in path $\mathcal{P} = \{v_i, v_j\}$, is given in (33), when the monitor is placed at node v_i .

$$\hat{w}_i = \sqrt{\frac{-b \pm \sqrt{b^2 - 4ac}}{2a}}. \quad (33)$$

where,

$$a = -3c - 24N_{00_i} - 24(N_i - N_{00_i}) \quad (34)$$

$$b = 24N_{00_i} - 8(N_i - N_{00_i}) + 2c \quad (35)$$

$$c = \sum_{j=2}^{m-1} \frac{24N_{00_j} k_j}{1 + 3k_j} - \frac{8(N_j - N_{00_j}) k_j}{1 - k_j}, \quad k_j = \frac{4N_{00_j} - N_j}{3N_j}. \quad (36)$$

Estimator \hat{w}_j is $\hat{w}_j = \frac{\sqrt{k_j}}{\hat{w}_i}$. Here, N_{00_j} is the number of outcomes in the state ϕ_{00} associated with link e_j , while N_j denotes the total number of measurements on that link.

Estimation Performance Analysis

Using the derived MLE estimators and the QCRB as a benchmark, we compare two- and three-monitor configurations in a four-node star network, where v_0 denotes the hub node and v_1, v_2 , and v_3 denote the end nodes to assess the impact of direct and indirect monitoring on estimation precision. We first benchmark the achievable estimation precision for different monitor placements using the QCRB. Fig. 5a presents the QCRB values of the estimators w_1, w_2 , and w_3 corresponding to the links $e_1 = (v_0, v_1)$, $e_2 = (v_0, v_2)$, and $e_3 = (v_0, v_3)$, under the two-monitor configuration with monitors placed at the nodes v_1 and v_2 . The results show that the QCRB values for w_1 and w_2 are identical, while the QCRB value for w_3 is significantly higher. This disparity reflects a lower estimation precision for w_3 , which is indirectly monitored. Fig. 5b displays the QCRB values for the same three estimators in a three-monitor configuration with monitors placed at the nodes v_1, v_2 , and v_3 . In this setup, the QCRB values for w_1, w_2 , and w_3 are equal, demonstrating uniform and improved estimation accuracy across all links when directly measured by the monitor.

We next analyze the finite-sample performance of the maximum likelihood estimators and their convergence toward the QCRB. Figs. 6a and 6b present the mean square error (MSE) of the MLEs as a function of the number of samples for network configurations with two and three monitors. The values of the Werner parameters w_1, w_2 , and w_3 are fixed at 0.9. The results indicate that the MSE decreases as the number of samples increases, demonstrating improved estimator accuracy with larger data sets. In the three-monitor setup, all estimators exhibit similar behavior and converge to the same value, suggesting uniform estimation accuracy across the network. In contrast, in the two-monitor setup, the estimator corresponding to the link without a directly connected monitor converges to a higher MSE compared to the other two

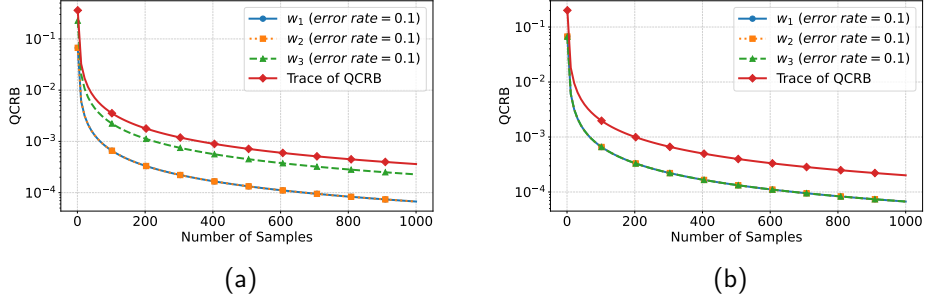


Fig. 5 Numerical Analysis using QFIM: (a) QCRB of the three estimators and QCRB trace, with error rate = 0.1 in two-monitor configuration, (b) QCRB of three estimators and trace of QCRB in Three-Monitor configuration for error rate = 0.1.

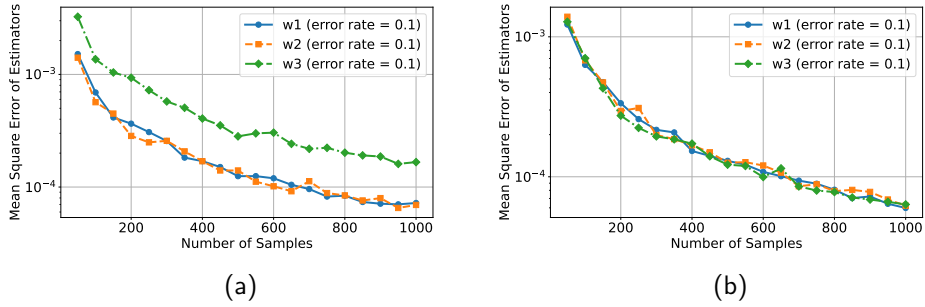


Fig. 6 Maximum Likelihood Estimator for Werner parameter: (a) Mean square error of MLE for Two Monitor Setup with error rate=0.1 for all three estimators, (b) Mean square error of MLE for Three-Monitor Setup with error rate=0.1 for all three estimators.

estimators, which are associated with links that have direct monitor connections. This observation aligns with our theoretical expectations, confirming that the presence of a monitor directly impacts estimation accuracy. Furthermore, the observed MSE trends closely resemble those in the QCRB plots shown in Figs. 5a and 5b, indicating that the estimators effectively approach the lower bound set by the QCRB.

Discussion

This study addresses the problem of Quantum Network Tomography by investigating how optimal monitor placement influences the precision of parameter estimation of quantum channels. We derived closed-form expressions for the MLE, for estimating Werner parameters of network links in an n -node quantum star network under different monitor configurations when network links are modeled as depolarizing channels. The QFIM expression holds for arbitrary networks, and numerical analysis using QCRB demonstrates that distributing monitors across multiple end nodes, particularly those

connected to the least noisy links in the network, substantially improves estimation accuracy. It also highlights the benefit of direct measurements in reducing estimation variance.

To enable scalable monitor placement in large quantum networks, we formulated the problem as an ILP. We proposed two objective formulations: one that jointly optimizes estimation accuracy with monitoring-overhead (QMF) and another that focuses exclusively on estimation accuracy (QF). Our evaluations on star networks show that the choice between the QMF and QF formulations ultimately depends on network requirements: the first approach is well suited for practical deployments where monitor resources are limited or load balancing is critical, whereas the second formulation is more appropriate when estimation accuracy is the primary objective, particularly in the presence of heterogeneous noise. We provided a faster algorithm to compute the solution of both QF and QMF on star networks, with formal proofs of correctness that remove the necessity of solving the ILPs for these particular topologies. In addition, we utilize our ILPs to solve optimal monitor placement on tree topologies, demonstrating its applicability to more general network structures.

Data Availability

All data generated and analyzed during the study are available from the corresponding author upon reasonable request.

Code Availability

The codes used for generating and analyzing data are available from the corresponding author upon reasonable request.

References

- [1] Paris, M. G. Quantum estimation for quantum technology. *International Journal of Quantum Information* **7**, 125–137 (2009).
- [2] Northup, T. & Blatt, R. Quantum information transfer using photons. *Nature photonics* **8**, 356–363 (2014).
- [3] He, T., Ma, L., Swami, A. & Towsley, D. *Network tomography: identifiability, measurement design, and network state inference* (Cambridge University Press, 2021).
- [4] Castro, R., Coates, M., Liang, G., Nowak, R. & Yu, B. Network tomography: Recent developments (2004).
- [5] Adams, A. *et al.* The use of end-to-end multicast measurements for characterizing internal network behavior. *IEEE Communications magazine* **38**, 152–159 (2000).

- [6] Jin, X., Yiu, W.-P. K., Chan, S.-H. G. & Wang, Y. Network topology inference based on end-to-end measurements. *IEEE Journal on Selected areas in Communications* **24**, 2182–2195 (2006).
- [7] He, T. *et al.* Robust monitor placement for network tomography in dynamic networks. *IEEE INFOCOM 2016-The 35th Annual IEEE International Conference on Computer Communications*, 1–9 (IEEE, 2016).
- [8] Ma, L., He, T., Leung, K. K., Swami, A. & Towsley, D. Monitor placement for maximal identifiability in network tomography. *IEEE INFOCOM 2014-IEEE Conference on Computer Communications*, 1447–1455 (IEEE, 2014).
- [9] Nielsen, M. A. & Chuang, I. L. *Quantum Computation and Quantum Information: 10th Anniversary Edition* (Cambridge University Press, Cambridge, 2010).
- [10] Iqbal, M., Ahmadian, M., Velasco, L. & Ruiz, M. Reliable quantum communication. *2023 23rd International Conference on Transparent Optical Networks (ICTON)*, 1–4 (IEEE, 2023).
- [11] De Andrade, M. G. *et al.* Quantum network tomography with multi-party state distribution. *2022 IEEE International Conference on Quantum Computing and Engineering (QCE)*, 400–409 (2022).
- [12] De Andrade, M. G., Navas, J., Montano, I. & Towsley, D. On the characterization of quantum flip stars with quantum network tomography. *2023 IEEE International Conference on Quantum Computing and Engineering (QCE)*, Vol. 1, 1260–1270 (IEEE, 2023).
- [13] De Andrade, M. G. *et al.* Quantum network tomography. *IEEE Network* **38**, 114–122 (2024).
- [14] Raghunadhan, A. K. *et al.* Measurement strategies and estimation precision in quantum network tomography. *arXiv preprint arXiv:2511.01657* (2025).
- [15] Raghunadhan, A. K. *et al.* Optimal monitor placement in quantum network tomography. *2024 IEEE International Conference on Quantum Computing and Engineering (QCE)*, Vol. 2, 370–371 (IEEE, 2024).
- [16] Liu, J., Yuan, H., Lu, X.-M. & Wang, X. Quantum fisher information matrix and multiparameter estimation. *Journal of Physics A: Mathematical and Theoretical* **53**, 023001 (2019).
- [17] Yu, M. *et al.* Quantum fisher information measurement and verification of the quantum cramer–rao bound in a solid-state qubit. *npj Quantum Information* **8**, 56 (2022).

- [18] Hervas, J. *et al.* Beyond the quantum cramer-rao bound. *Physical Review Letters* **134**, 010804 (2025).
- [19] Myung, I. J. Tutorial on maximum likelihood estimation. *Journal of mathematical Psychology* **47**, 90–100 (2003).
- [20] Barnum, H., Nielsen, M. A. & Schumacher, B. Information transmission through a noisy quantum channel. *Physical Review A* **57**, 4153 (1998).
- [21] Schumacher, B. Sending entanglement through noisy quantum channels. *Physical Review A* **54**, 2614 (1996).
- [22] Burrell, C. K. Geometry of generalized depolarizing channels. *Phys. Rev. A* **80**, 042330 (2009).
- [23] Sen(De), A., Sen, U., Brukner, Č., Bužek, V. & Żukowski, M. Entanglement swapping of noisy states: A kind of superadditivity in nonclassicality. *Physical Review A* **72** (2005).
- [24] Verma, V. & Prakash, H. *Quantum teleportation of single qubit mixed information using werner-like state as resource. 12th International Conference on Fiber Optics and Photonics*, S5A.82 (Optica Publishing Group, 2014).
- [25] Lee, J. & Kim, M. S. Entanglement teleportation via werner states. *Phys. Rev. Lett.* **84**, 4236–4239 (2000).
- [26] Bowen, G. & Bose, S. Teleportation as a depolarizing quantum channel, relative entropy, and classical capacity. *Phys. Rev. Lett.* **87**, 267901 (2001).
- [27] Bruss, D., Faoro, L., Macchiavello, C. & Palma, G. M. Quantum entanglement and classical communication through a depolarizing channel. *Journal of Modern Optics* **47**, 325–331 (2000).
- [28] Fiurášek, J. Maximum-likelihood estimation of quantum measurement. *Physical Review A* **64**, 024102 (2001).
- [29] Mwangi, W. P., Anapapa, A. & Otieno, A. Selection of second order models' design using d-, a-, e-, t- optimality criteria. *Asian Journal of Probability and Statistics* **5**, 1–15 (2019).
- [30] Rady, E., Abd El-Monsef, M. & Seyam, M. Relationships among several optimality criteria. *Interstat* **15**, 1–11 (2009).
- [31] Atkinson, A. C., Donev, A. N. & Tobias, R. D. in *Optimum experimental design with sas Optimum Experimental Designs, with SAS* (Oxford University Press, 2007).

- [32] Vickers, N. A. & Andersson, S. B. Information optimal control for single particle tracking microscopy. *IFAC-PapersOnLine* **54**, 649–654 (2021). 19th IFAC Symposium on System Identification SYSID 2021.
- [33] Ballo, G., Hangos, K. M. & Petz, D. Convex optimization-based parameter estimation and experiment design for pauli channels. *IEEE Transactions on Automatic Control* **57**, 2056–2061 (2012).
- [34] Ruppert, L., Virosztek, D. & Hangos, K. Optimal parameter estimation of pauli channels. *Journal of Physics A: Mathematical and Theoretical* **45**, 265305 (2012).

Acknowledgements

This research was supported by Research Ireland grant 21/US-C2C/3750 for CoQREATE (Convergent Quantum REsearch Alliance in Telecommunications), CONNECT-2 grant 13/RC/2077-P2, and by the NSF-ERC Center for Quantum Networks grant EEC- 1941583.

Author contributions

A.K.R. and M.G.A. contributed equally to this work. N.M., D.T., D.K., and I.D. provided supervision and guidance throughout this project. All authors contributed to the discussions and to the refinement of the manuscript.

Competing interests

The authors declare no competing interests.

Additional information

Supplementary information